Original Article
Downregulation of LINC01021 by curcumin analog Da0324 inhibits gastric cancer progression through activation of P53

Fanfan Xu[2], Ziwei Ji[2], Leye He[2], Mengxia Chen[2], Hao Chen[2], Qian Feng[2], Buyuan Dong[2], Xingyi Yang[2], Lei Jiang[1], Rong Jin[2,3]

[1]Central Laboratory, Departments of [2]Gastroenterology, [3]Epidemiology, The First Affiliated Hospital of Wenzhou Medical University, Wenzhou 325000, China

Abstract: Curcumin is a safe, cost-effective natural agent with multiple targets that displays therapeutic potential in cancer. Recently, we reported a novel curcumin analog, Da0324, which exhibited significantly improved stability and anti-cancer activity. However, the molecular mechanism underlying the anti-cancer activity of Da0324 remains largely unknown. Long non-coding RNAs have been shown to play important roles in cancer development and progression and may be potential targets for cancer therapy. Here, we showed that Da0324 treatment down-regulated the expression of *LINC01021* in gastric cancer cells. Da0324 treatment or knockdown of *LINC01021* by antisense oligos significantly inhibited gastric cancer cell growth, and also up-regulated P53 expression and down-regulated Bcl-2 expression *in vitro* and *in vivo*. Furthermore, Da0324 treatment or knockdown of *LINC01021* in gastric cancer cells suppressed cell migration, invasion and epithelial-mesenchymal transition (EMT), as well as induced apoptosis and autophagy. In addition, overexpression of *LINC01021* promoted growth and EMT, inhibited P53 expression and increased Bcl-2 expression in gastric cancer cells. Finally, overexpression of *LINC01021* reversed the anti-cancer effect of Da0324. Our findings indicate a novel anti-cancer mechanism for Da0324, and that *LINC01021* might be a potential therapeutic target for the treatment of gastric cancer.

Keywords: Curcumin analog, Da0324, gastric cancer, *LINC01021*

Introduction

Gastric cancer (GC) is one of the most common malignant tumors in the world and has high mortality [1, 2]. As methods of GC prevention and treatment have developed, the incidence of GC has been reduced, but it still remains one of the leading causes of cancer-related mortality in Asia [3]. One of the main treatments for GC is surgery, but most patients with early GC have a low rate of radical resection and a high recurrence rate [4]. Another major treatment option is chemotherapy, but its long-term application is likely to produce body resistance [5, 6]. Therefore, there is an urgent need to develop new therapeutic targets and drugs for GC.

Long non-coding RNAs (lncRNAs) are defined as RNAs greater than 200 bases in length that have no obvious coding ability [7]. Recent anal-

yses indicate that the human genome encodes approximately 32,000 lncRNAs, and that these play critical roles in various cellular and physiological functions [8]. LncRNAs affect gene regulation through a variety of mechanisms, but their main function is realized through interaction with RNA, DNA or protein [9]. Cytoplasmic lncRNAs bind to and regulate proteins or RNAs, some have been proposed to act as "miRNA sponges", adsorbing and inactivating specific miRNAs, while others can work as scaffolds, combining with proteins to form complexes [9, 10]. Nuclear-retained lncRNAs cooperate with proteins for the *cis-* or *trans*-regulation of chromatin status, which also directs proteins to specific genomic regions [11, 12]. Accordingly, lncRNAs regulate a variety of cellular functions, including chromatin remodeling, transcription, mRNA precursor splicing, and RNA stability [10, 13, 14]. Accumulating evidence demonstrated

that dysregulation of lncRNAs occurs in a variety of human cancers, and lncRNAs have been found to participate in GC development and progression [15]. Ultimately, lncRNAs have been revealed as a novel, potential therapeutic target for the treatment of cancer [16].

Since the application of chemotherapy to cancer treatment, natural compounds have become an important class of anti-tumor drugs [17]. Curcumin is an ancient spice and herb that is extracted from the roots of turmeric plants, part of the ginger's family [18]. Curcumin has been received attention for its many biological activities, such as anti-inflammatory [19, 20], antioxidant [21, 22] and anti-tumor [21, 23], which are realized either alone or in combination with drugs [24]. Unfortunately, the therapeutic potential of curcumin is limited by its low bioavailability, chemical instability and rapid metabolism [25]. A potentially effective strategy for solving these difficulties in the application of curcumin is to design a structural analog with superior pharmacokinetic and biological properties. In our previous study, we discovered a promising curcumin analog named Da0324, which displayed target selectivity for GC cells with improved stability and inhibited NF-KB activation in GC cells [26]. However, the molecular mechanisms underlying the anti-cancer activities of Da0324 are still not fully understood. In the present study, we report that Da0324 exerts anti-tumor activities against GC through downregulation of *LINC01021*. This finding provides an important direction for the development of clinical anticancer drugs and targeted therapies.

Materials and methods

Cell lines and culture

The human GC cell line KATO III and the human normal gastric mucosa epithelial cell line GES-1 were obtained from the Cell Bank of the Chinese Academy of Science (Shanghai, China). The cell lines BGC-823 and SGC-7901 were purchased from the China Center for Type Culture Collection (Wuhan, China). All cell lines were grown in RPMI-1640 medium (Thermo Fisher Scientific, Waltham, MA, USA) supplemented with 100 U/mL penicillin, 10 mg/L streptomycin (Thermo Fisher Scientific), and 10% fetal bovine serum (FBS) (Sigma, Germany). All cells

were cultured and maintained in a humidified incubator at 37°C under 5% CO_2 atmosphere.

High-throughput sequencing of lncRNAs

A high-throughput sequencing assay was performed to screen differentially expressed lncRNAs among total RNAs extracted from SGC7901 cells treated with either DMSO or 4 µM Da0324 for 48 h in triplicate. In brief, total RNA was extracted using TRIzol® reagent (Thermo Fisher Scientific) and ribosomal RNA was depleted with the Epicentre Ribo-Zero Gold kit according to the manufacturer's protocol (Illumina, San Diego, CA, USA). RNA fractions were fragmented into small pieces and then reverse-transcribed to create a complementary DNA (cDNA) library using the mRNA-Seq sample preparation kit (Illumina). Paired-end sequencing was performed using an Illumina HiSeq4000 sequencer (Illumina) by the service provider LianChuan Sciences (Hangzhou, China). Among differentially expressed lncRNAs, $\log_2$ (fold change) > 1 or $\log_2$ (fold change) < -1 with *P*-value < 0.05 was considered statistically significant.

Analysis of data from The Cancer Genome Atlas (TCGA)

LncRNA expression data from of 375 GC tissue samples and 32 normal stomach tissue samples were collected from the TCGA stomach adenocarcinoma dataset (STAD) and the level of *LINC01021* expression determined.

Cell transfection

Antisense oligos (ASOs) targeting *LINC01021* and siRNAs targeting P53, as well as corresponding negative controls (NC), were synthesized by RiboBio Biotech (Guangzhou, China). The oligo sequences were *LINC01021*-ASO-1: 5'-CCT GCG CAT ATT TAA CTA TC-3'; *LINC01021*-ASO-2: 5'-GTT CTT AAC CTG CGC ATA TT-3'; P53-siRNA: 5'-GAC TCC AGT GGT AAT CTA C-3'. The plasmid pcDNA-*P53* was used to overexpress *P53* in BGC823 and SGC7901 cells. Cell transfection was performed using Lipofectamine 3000 (Thermo Fisher Scientific) according to the manufacturer's instructions. Full-length *LINC01021* was amplified and cloned into the lentiviral vector plasmid pLVX-Puro (Clontech, Mountain View, CA, USA) between the EcoRI and BamHI restriction enzyme recognition

sites. Lentiviral particles were produced by co-transfection of HEK293T cells with pLVX-*LINC01021*, pMD2.G, pMDL-G/P-RRE and pRSV-REV [27].

Quantitative real-time PCR (qRT-PCR)

Total RNA was extracted using TRIzol® reagent (Thermo Fisher Scientific). For detection of the subcellular distribution of *LINC01021*, cyto-plasmic and nuclear RNA were isolated by PARIS™ Kit (Thermo Fisher Scientific). Total RNA was reverse transcribed to cDNA using the Revert Aid First-Strand cDNA Synthesis Kit (Thermo Fisher Scientific). For *LINC01021*, reverse transcription was performed with the InRcute lncRNA First-Strand cDNA Synthesis Kit (Tiangen, China). Quantitative PCR was performed on a CFX96 Real-time PCR system (Bio-Rad, Berkeley, CA, USA) using SYBR Premix Ex Taq (Takara, Japan). The relative *LINC01021* expression was calculated by a $2^{-\Delta\Delta Ct}$ method. U6 was used as an internal reference. The specific primer sequences are: *LINC01021*-forward: 5'-GGA ACC CCT CTT GCT TTG CA-3', *LINC01021*-reverse: 5'-ACG GGC ACA TTG AAG GGT CA-3'; U6-forward: 5'-CGC TTC ACG AAT TTG CGT GTC AT-3', U6-reverse: 5'-CGC TTC ACG AAT TTG CGT GTC AT-3'.

Western blot analysis

Proteins were extracted from GC cells or xeno-graft tumor tissues using radioimmunoprecipi-tation assay (RIPA) lysis buffer supplemented with phenylmethylsulfonyl fluoride, phospha-tase inhibitor and protease inhibitor. Proteins were resolved by sodium dodecyl sulfate-poly-acrylamide gel electrophoresis (SDS-PAGE) and transferred to polyvinylidene fluoride mem-branes. After that, the membranes were blocked with 5% skim milk at room temperature for 2 h and further incubated at 4°C overnight with specific primary antibodies against E-cadherin, N-cadherin, Bcl-2 (Santa Cruz Biotechnology, Santa Cruz, CA, USA), vimentin (BD Biosciences, San Jose, CA, USA), P53, LC3B, P62, p-mTOR, mTOR, GAPDH, and β-actin (Cell Signaling Technology, Bioke, The Netherlands). GAPDH or β-actin was used as an internal control. Then, the membranes were successively incubated with secondary anti-bodies (Santa Cruz Biotechnology) and ECL reagent. Finally, specific bands were detected

and analyzed by a scanning imaging system (Bio-Rad).

Cell viability and proliferation assays

For the CCK-8 assays, GC cells (5000 cells per well) were seeded into 96-well plates and incu-bated in RPMI-1640 medium containing differ-ent dosages of Da0324 for 24 h, 48 h, or 72 h. CCK-8 solution (10 µl/well, Dojindo, Japan) was added to each well at 2 h before the indicated time point, and the absorbance was measured at 450 nm according to the manufacturer's pro-tocols. For clone formation assays, transfected or Da0324-treated cells were seeded in six-well plates (800 cells/well) and cultured for two weeks. At the end of the experiment, cells were fixed with 4% paraformaldehyde and stained with crystal violet solution. Colony numbers were used to assess cell proliferation.

Apoptosis assay

In brief, after treatment with Da0324 (4 µM) or transfection for 48 h, cells were harvested and then stained with Annexin V-FITC and propidi-um iodide (PI) using an Annexin V-FITC/PI Apoptosis Detection Kit (BD Biosciences). Cell apoptosis was assessed by flow cytometry According to the manufacturer's instructions (FACSCalibur, Becton Dickinson, Franklin Lakes, NJ, USA).

Cell migration and invasion assays

The migratory and invasive abilities of GC cells were evaluated using a transwell chamber with or without matrigel coating (BD Bioscience). GC cells (5×10^5 cells/well) were seeded in the upper chamber in RPMI-1640 medium without FBS and treated with Da0324, while 800 µL culture medium containing Da0324 and 10% FBS was added to the lower chamber. After incubation for 24 h at 37°C, the transwell chambers were successively fixed with 4% paraformaldehyde for 30 min and stained with crystal violet for another 30 min. Five random fields were counted per chamber using a microscope.

Animal experiments

Female BALB/c-nu mice (4-5 weeks old) were prepared for making a xenograft model. After resuspension in PBS, KATO III cells (5×10^6

cells/mouse) were injected subcutaneously into the right dorsal flank of the nude mice. When the tumor volume reached approximately 50 mm^3, the nude mice were randomized into four groups that received the following treatments: (1) PBS as vehicle control (n = 6); (2) Da0324 (dissolved in 6% castor oil and 94% PBS, 20 mg/kg, n = 6); (3) ASO-control (dissolved in PBS, 250 nmol/kg, n = 5); (4) ASO-*LINC01021* (dissolved in PBS, 250 nmol/kg, n = 5). Vehicle or Da0324 was given via intraperitoneal injection every day for 18 days. ASO-control and ASO-*LINC01021* were administered through intratumoral injection at three-day intervals, and the ASO-control treatment was used as a control group. Tumors were excised after 24 days of treatment. Tumor volumes and animal body weights were measured and recorded every other day. Tumor volumes were calculated according to the following formula: volume = 0.5×L×W^2 (L, longest diameter; W, diameter perpendicular to the longest diameter). At the end of the treatment, the mice were euthanized, and the xenograft tumors were dissected and weighed. All operations for animal experiments were approved by the Animal Experimental Ethics Committee of Wenzhou Medical University.

Statistical analysis

All statistical analyses were carried out using GraphPad Prism7.0 (GraphPad Prism, Inc., La Jolla, CA, USA). Student's *t*-test was used to analyze differences between two groups. One-way analysis of variance was used to calculate statistical significance of differences between three groups. The results were expressed as means ± SD. A *P*-value < 0.05 was considered statistically significant.

Results

Da0324 inhibits proliferation and induces apoptosis and autophagy in GC cells

To verify whether Da0324 exhibited a cytostatic effect of GC cells, CCK-8 assays were performed to assess cell viability in response to Da0324 treatment in BGC823, SGC7901 and KATO III GC cells. The results showed that Da0324 significantly reduced the viability of all three cell lines in a time- and dose-dependent manner (**Figure 1A**), At 48 h to Da0324 exposure, the half maximal inhibitory concen-

tration (IC50) values were 3.48 ± 0.59, 3.72 ± 0.20 and 4.69 ± 0.02 µM for BGC823, SGC7901, and KATO III cells, respectively (**Figure 1B**). Consistently, proliferation of GC cells was inhibited with Da0324 treatment, as evidenced by reduced colony formation (**Figure 1C**). In addition, the apoptosis-inducing effects of Da0324 were examined using Annexin-V/PI double staining. As shown in **Figure 1D**, Da0324 induced significant apoptotic effects in BGC823, SGC7901 and KATO III cells. The pro-apoptotic effect of Da0324 was supported by increased expression levels of P53 and decreased expression of the apoptosis-related protein Bcl-2 in Da0324-treated cells (**Figure 1E**). To test whether Da0324 treatment induced autophagy in GC cells, we analyzed the specific autophagy markers microtubule-associated protein light chain3B (LC3B) and P62 along with the autophagy-associated proteins mTOR and phosphorylated mTOR (p-mTOR) by western blotting. The LC3B protein has two variants: LC3B-I and LC3B-II, and turnover of LC3B-I to LC3B-II is considered a hallmark of autophagy [28]. As indicated in **Figure 1E**, protein levels of p-mTOR and P62 were reduced and the ratio of LC3B-II/LC3B-I was elevated in BGC823 and SGC7901 cells treated with Da0324, suggesting that Da0324 could induce autophagy in GC cells.

Da0324 inhibits migration, invasion, and epithelial-mesenchymal transition (EMT) in GC cells

The effects of Da0324 on migration and invasion of GC cells were assessed with transwell assays, in which Da0324 significantly inhibited the migration and invasion of BGC-823, SGC7901 and KATO III cells (**Figure 2A**). EMT is important for tumor migration and invasion, thus the effect of Da0324 on the expression of EMT markers in GC cells was also analyzed by western blotting. As shown in **Figure 2B**, Da0324 treatment of GC cells increased expression of E-cadherin and decreased expression of N-cadherin and vimentin.

Da0324 treatment suppresses long non-coding RNA LINC01021 expression in GC cells

High-throughput sequencing was used to identify differentially expressed lncRNAs in SGC-7901 cells treated with DMSO (control) or 4 µM Da0324 for 48 h. A total of 280 differentially
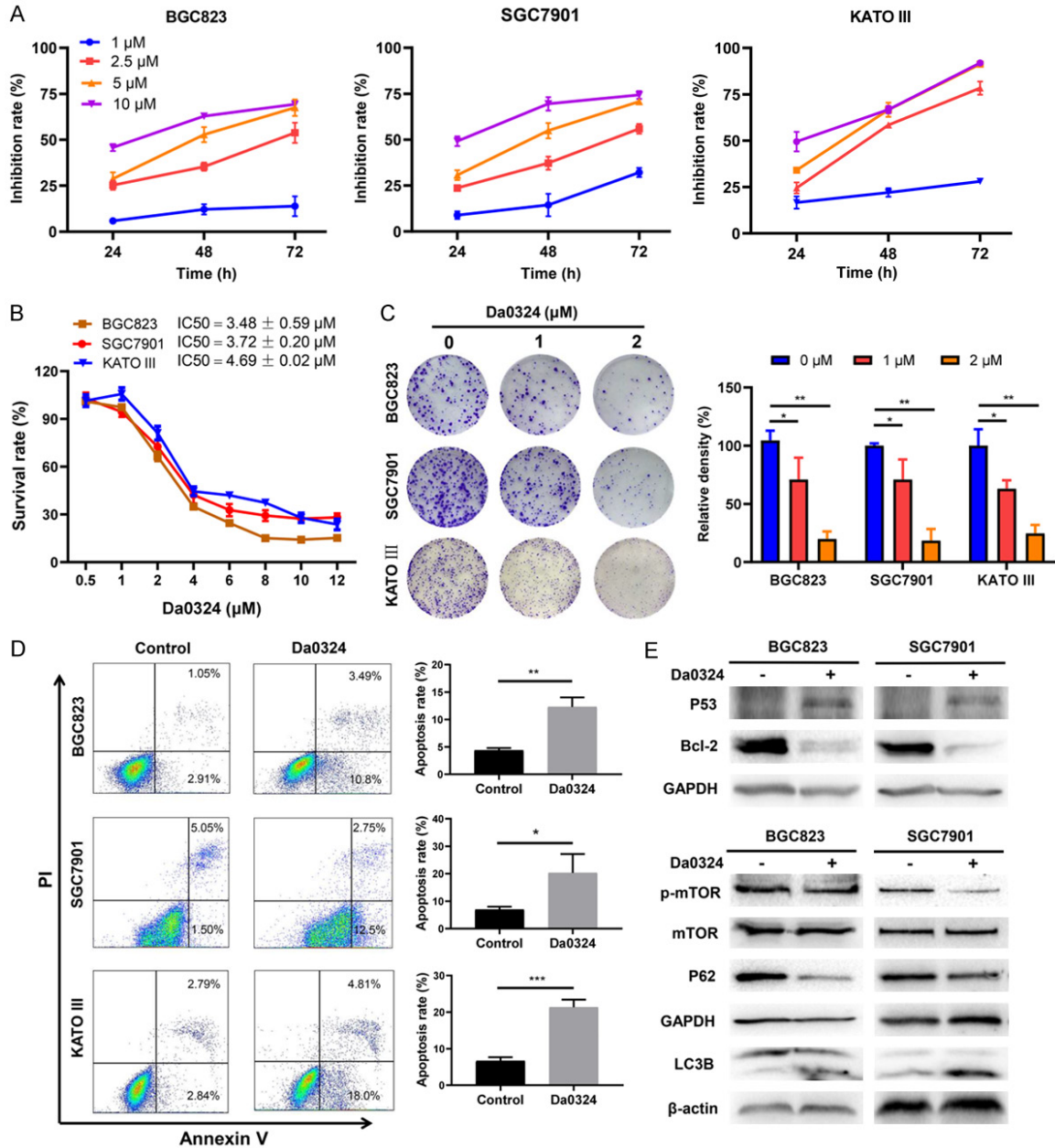
Figure 1. Da0324 inhibits proliferation and induces apoptosis and autophagy in gastric cancer cells. A. Gastric cancer cell lines (BGC823, SGC7901 and KATO III) were treated with the indicated concentration of Da0324 for 24 h, 48 h, or 72 h. Cell viability was measured using a Cell Counting Kit-8 (CCK-8) and Growth inhibition rates of Da0324 on GC cells were in comparison with untreated cells. B. BGC823, SGC7901 and KATO III cells were treated with 0, 0.5, 1, 2, 4, 6, 8, 10, or 12 mM Da0324 for 48 h, and cell viability was measured by CCK-8 assays. The half maximal inhibitory concentration (IC50) values were calculated with GraphPad statistical software. C. Clonogenic assay showed the effects of Da03224 treatment on clonogenic formation in gastric cancer cells. BGC823, SGC7901 and KATO III cells were treated with Da0324 (1 or 2 μM) for 48 h, then cultured for two weeks in complete medium and the colony density calculated. Representative images of clonogenic assay (left panel) and quantitative analysis (right panel). All data are representative of three independent experiments and are presented as the means ± SD. *, $P < 0.05$; **, $P < 0.01$. D. BGC823, SGC7901 and KATO III cells were treated with 4 μM Da0324 for 48 h. Cells were fixed and stained with Annexin V/PI and apoptosis was analyzed by flow cytometry. Representative dot plots of Annexin V/PI staining are shown in the left panel, and quantitative data are presented in the right panel. All data are representative of three independent experiments and are presented as the means ± SD. *, $P < 0.05$; **, $P < 0.01$; ***, $P < 0.001$. E. BGC823 and SGC7901 cells were treated with 4 μM Da0324 or control for 48 h and then harvested for analysis by western blot using P53, Bcl-2, p-mTOR, mTOR, P62, and LC3B antibodies. GAPDH or β-actin was used as an internal control.
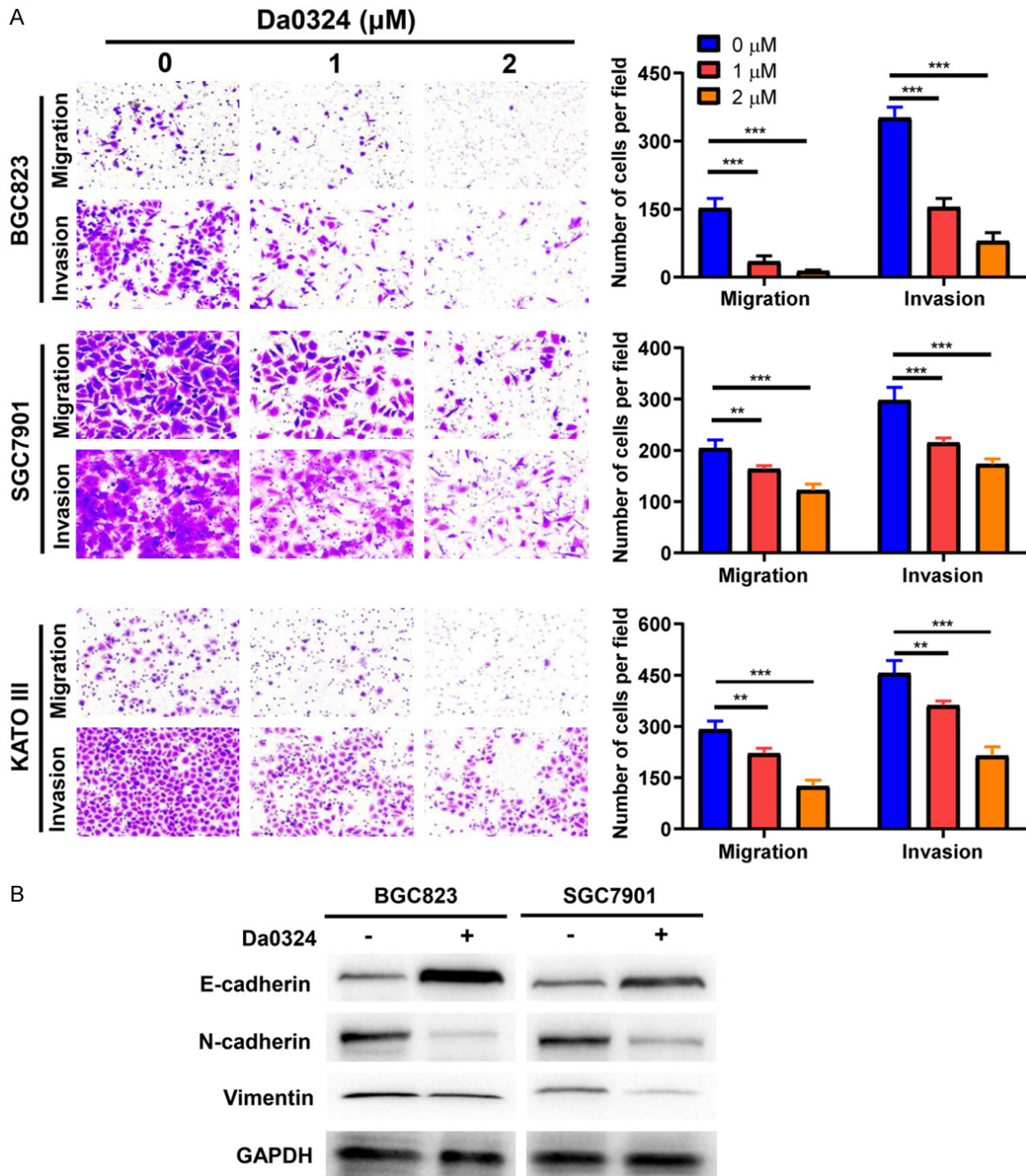
Figure 2. Da0324 inhibits migration, invasion, and EMT in GC cells. A. BGC823, SGC7901 and KATO III cells were treated with Da0324 (1 or 2 µM) for 24 h and transwell migration and matrigel invasion assays were performed. Representative image (left panel) and quantitative data (right panel) of cell migration and invasion are shown. Bar graphs are representative of three independent experiments and the data are presented as the means ± SD. **, $P < 0.01$; ***, $P < 0.001$. B. Western blot analysis for the expression of E-cadherin, vimentin, and N-cadherin in BGC823 and SGC7901 cells treated with or without 2 µM Da0324. GAPDH was used as an internal control.

expressed lncRNAs were identified (152 upregulated and 128 downregulated, $P < 0.05$, fold change > 2 or < -2) (**Figure 3A**). **Figure 3B** shows the top 40 most significantly differentially expressed lncRNAs. To verify the consis-tency of the lncRNA sequence data, ten lncRNAs were selected for qRT-PCR analysis, of which eight were validated (**Figure 3C**). LI-NC01021 was amongst the most highly down-regulated lncRNAs, and was selected for fur-
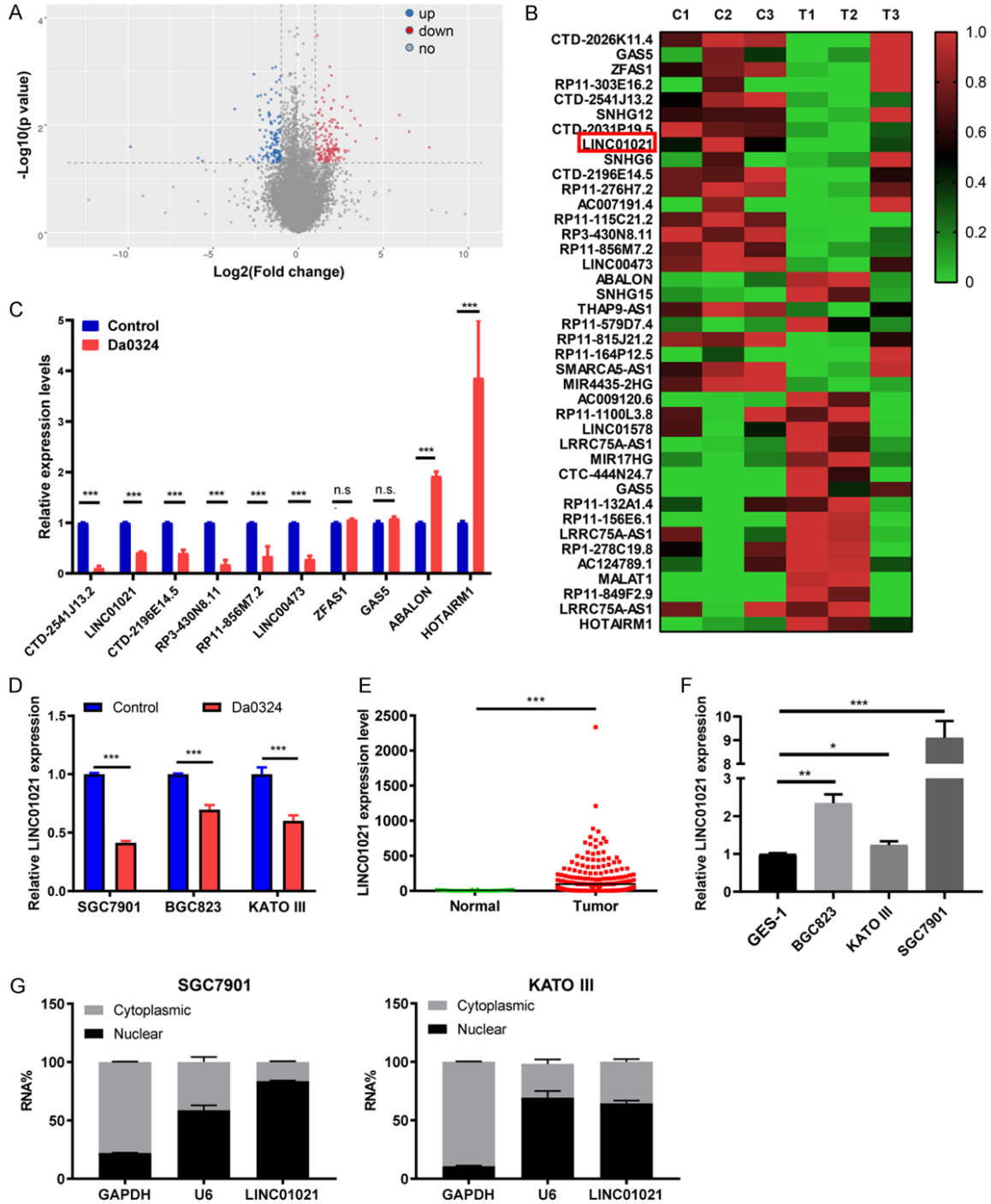
Figure 3. Long non-coding RNA *LINC01021* was downregulated by Da0324 treatment in gastric cancer cells. A. Volcano plots of lncRNAs differentially expressed between the control and Da0324 treatment groups. SGC7901 cells were treated with DMSO (control) or 4 μM Da0324 for 48 h and high-throughput sequencing assay was performed. The X-axis represents $\log_2$ of fold changes. The Y-axis represents $-\log_{10}$ of P values. Red spots denote upregulated lncRNAs, blue spots denote downregulated lncRNAs. B. Heatmap of the top 40 lncRNAs most significantly differentially expressed in SGC7901 cells with Da0324 treatment. C. Ten differentially expressed lncRNAs regulated by Da0324 were validated by qRT-PCR. SGC7901 cells were treated with DMSO (control) or 4 μM Da0324 for 48 h. RNAs were isolated and converted to cDNA. Quantitative real-time PCR was performed to determine the expression level of lncRNAs. GAPDH was used as a housekeeping gene. All bars represent relative expression levels and data represent mean ± SD. ***, $P < 0.001$; n.s. means no significant difference. D. *LINC01021* expression by qRT-PCR in BGC823, SGC7901 and KATO III cells treated with Da0324 or DMSO (control) for 48 h. All bars represent relative

expression levels and data represent mean ± SD. ***, *P* < 0.001. E. TCGA data for the expression of *LINC01021* in gastric cancer tissues (n = 375) and normal tissues (n = 32). F. *LINC01021* expression by qRT-PCR in the normal gastric epithelial cell line GES-1 and in gastric cancer cell lines (BGC823, SGC7901, and KATO III). All bars represent relative expression levels and data represent mean ± SD. *, *P* < 0.05; **, *P* < 0.01; ***, *P* < 0.001. G. The sub-cellular location of LINC01021 in SGC7901 and KATO III cells was determined by qRT-PCR. GAPDH was used as a positive control for cytoplasmic RNA localization, U6 for nuclear RNAs. The data are shown as means ± SD. lncRNA, long non-coding RNA; qRT-PCR, quantitative reverse transcription-polymerase chain reaction.

ther study based on the following considerations. First, expression of *LINC01021* was significantly downregulated in BGC823, SGC-7901 and KATO III cells treated with Da0324 for 48 h (**Figure 3D**). Second, according to data from TCGA, *LINC01021* was remarkably overexpressed in GC tissues and cells when compared with normal tissues and normal gastric epithelial cells (**Figure 3E** and **3F**). Finally, qRT-PCR of cytoplasmic and nuclear fractions from GC cells indicated that most *LINC01021* was present in the nucleus (**Figure 3G**).

ASO-mediated silencing of LINC01021 inhibits cell proliferation and induces apoptosis and autophagy in GC cells

To explore the biologic roles of *LINC01021* in GC, we knocked down *LINC01021* in BGC823, SGC7901, and KATO III cells by transfection with ASOs specific for *LINC01021*. The knockdown efficiency of *LINC01021*-specific ASO-1 and *LINC01021*-specific ASO-2 was verified by qRT-PCR (**Figure 4A**). Growth curves generated from CCK-8 assays revealed that the ablation of *LINC01021* by *LINC01021*-specific ASO-1 and ASO-2 inhibited the growth of all three GC cell lines (**Figure 4B**). Similarly, knockdown of *LINC01021* decreased the clonogenic survival of BGC823 and SGC7901 cells in colony formation assays (**Figure 4C**). As apoptosis is a contributing factor for cancer cell growth inhibition, we evaluated apoptosis by flow cytometry analysis and found that BGC823 and SGC7901 cells transfected with *LINC01021*-specific ASO-1 and ASO-2 had higher apoptotic rates than did the same cells transfected with ASO-control (**Figure 4D**), demonstrating that knockdown of *LINC01021* induced apoptosis in GC cells. Moreover, BGC823 and SGC7901 cells transfected with *LINC01021*-specific ASO-1 and ASO-2 expressed significantly higher levels of P53 and lower levels of Bcl-2 protein (**Figure 4E**). Knockdown of *LINC01021* also increased the conversion of LC3B-I into LC3B-II, and decreased the levels of P62 and phosphorylation of mTOR (**Figure 4F**). These data confirm that reduced expression of *LINC01021* inhibits cell growth and promotes apoptosis and autophagy in GC cells *in vitro*.

ASO-mediated silencing of LINC01021 inhibits GC cell migration, invasion, and EMT

Next, we performed transwell assays to determine the migration and invasion capacity of BGC823 and SGC7901 cells following *LINC01021* knockdown. We observed that the migratory and invasive properties of both cell lines were significantly impaired after knockdown with *LINC01021*-specific ASO-1 and ASO-2 (**Figure 5A**). Additionally, as determined by western blotting of EMT-related markers, *LINC01021* knockdown increased E-cadherin protein expression level and inhibited N-cadherin and vimentin protein expression (**Figure 5B**).

Da0324 or LINC01021-specific ASO treatment suppresses tumor growth of human GC xenografts in vivo

To investigate whether Da0324 inhibited tumor growth *in vivo*, KATO III cells were used to create a subcutaneous xenograft model in nude mice. As shown in **Figure 6A** and **6B**, relative to the control group, treatment with Da0324 substantially reduced the volume, size, and weight of tumors in KATO III xenografted mice. Meanwhile, there was no significant difference in body weight between the control group and the Da0324 treatment group, indicating no apparent toxicity of Da0324 *in vivo* (**Figure 6C**). Results from qRT-PCR showed that Da0324 treatment downregulated expression of *LINC01021* (**Figure 6D**). In addition, Da0324 treatment significantly upregulated the protein expression of P53 and suppressed the expression of Bcl-2 (**Figure 6E**). To determine whether *LINC01021* affected tumorigenesis, KATO III cells were inoculated subcutaneously into nude mice and ASOs administered by intratumoral injection. Both xenograft tumor weight and vol-
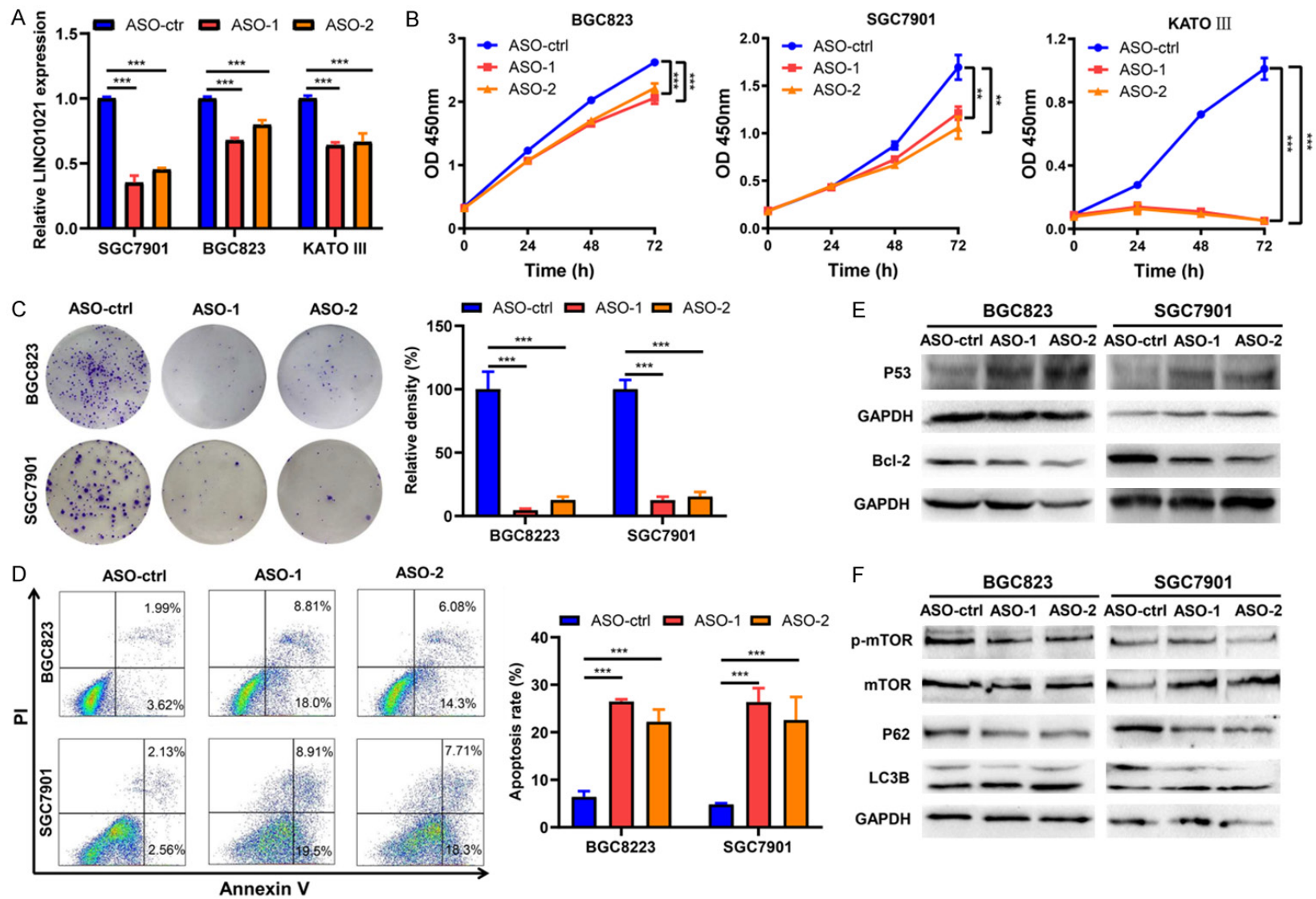
Figure 4. ASO-mediated silencing of *LINC01021* inhibits cell proliferation and induces apoptosis and autophagy in gastric cancer cells. A. BGC823, SGC7901 and KATO III cells were transfected with 50 nM ASO-control, *LINC01021*-specific ASO-1, or *LINC01021*-specific ASO-2 for 48 h. *LINC01021* expression were determined by qRT-PCR. B. BGC823, SGC7901 and KATO III cells were transfected with 50 nM ASO-control, *LINC01021*-specific ASO-1, or *LINC01021*-specific ASO-2. At 0, 24, 48 or 72 h post-transfection, cell viability was determined by the CCK-8 assays. The data were expressed as mean ± SD. All data are representative of three independent experiments. **, $P < 0.01$; ***, $P < 0.001$. C. The proliferation of gastric cancer cells (BGC823 and SGC7901) transfected with *LINC01021*-ASOs

or ASO-control was determined by colony formation assays. The data were expressed as mean ± SD. All data are representative of three independent experiments. **, *P* < 0.01; ***, *P* < 0.001. D. Flow cytometry analysis of cell apoptosis in gastric cancer cells (BGC823 and SGC7901). Cells were transfected with 50 nM *LINC01021*-ASOs or ASO-control for 48 h and stained with Annexin V/PI. Representative dot plots of Annexin V/PI staining are shown in the left panel, and quantitative data are presented in the right panel. All data are representative of three independent experiments and are presented as the means ± SD. ***, *P* < 0.001. E, F. Western blot analysis of P53, Bcl-2, mTOR, p-mTOR, P62, and LC3B expression in BGC823 and SGC7901 cells transfected with *LINC01021*-ASOs or ASO-control. qRT-PCR, quantitative reverse transcription-polymerase chain reaction; ASO, antisense oligo; LC3B, light chain3B; p-mTOR, phosphorylated mTOR.
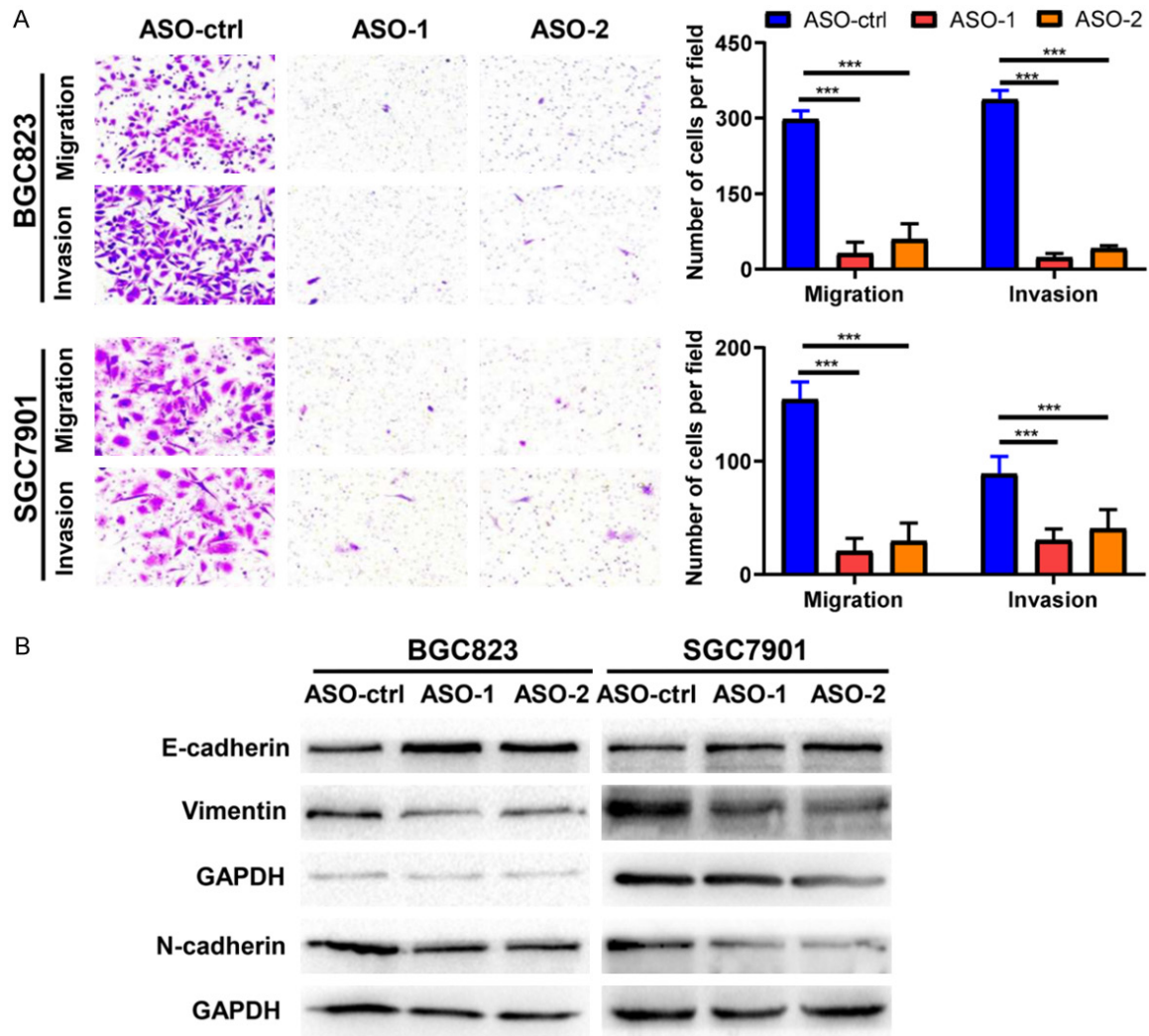
Figure 5. ASO-mediated silencing of *LINC01021* inhibits gastric cancer cell migration, invasion, and EMT. A. BGC823 and SGC7901 cells were transfected with 50 nM ASO-control, *LINC01021*-specific ASO-1 or *LINC01021*-specific ASO-2 for 48 h and transwell migration and matrigel invasion assays were performed. Representative image (left panel) and quantitative data (right panel) of cell migration and invasion are shown. All data are presented as the means ± SD. ***, *P* < 0.001. B. Western blot analysis of the expression of E-cadherin, N-cadherin and vimentin proteins in BGC823 and SGC7901 cells transfected with ASO-control, *LINC01021*-specific ASO-1 or *LINC01021*-specific ASO-2. ASO-ctrl, ASO-control; EMT, epithelial-mesenchymal transition.

ume were remarkably reduced in the ASO-*LINC01021* treatment group when compared to the control group (**Figure 6F** and **6G**). As shown in **Figure 6H**, ASO-*LINC01021* treatment does not affect the weight of nude mice. Furthermore, qRT-PCR confirmed that ASO-*LINC01021* treatment suppressed the expression of *LINC01021* in tumor tissues (**Figure 6I**).
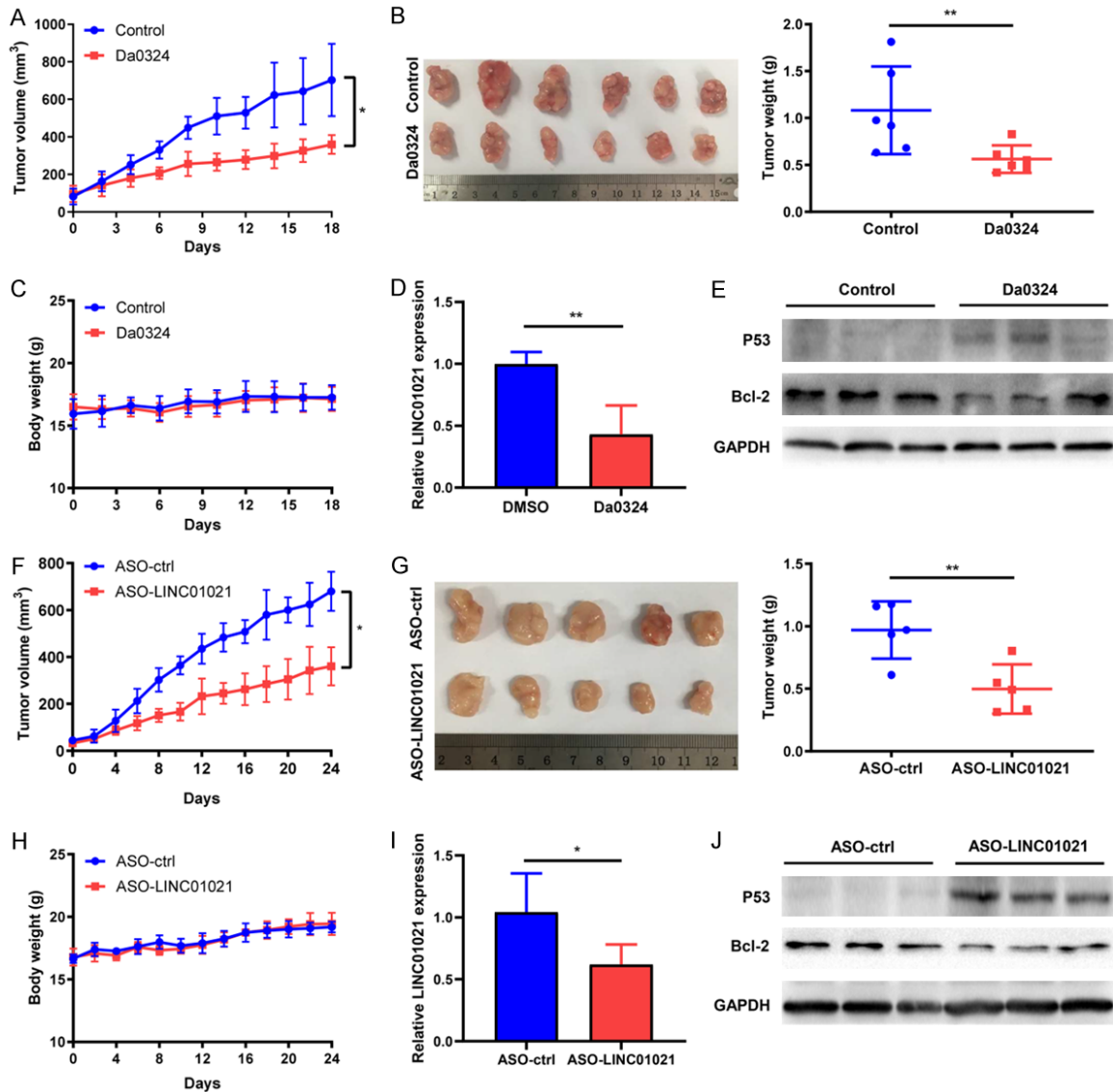
Figure 6. Da0324 or *LINC01021*-specific ASO treatment suppresses tumor growth of GC cells *in vivo*. A. Effects of Da0324 treatment on tumor volume in subcutaneous xenograft mouse models using KATO III cells. Tumor volume as measured by caliper of Da0324 (20 mg/kg, intraperitoneal injection every day) or vehicle administered for 18 days in a subcutaneous xenograft model. The data were expressed as mean ± SD. *, $P < 0.05$. B. Tumors were excised after 18 days of treatment. Images and weight of the dissected xenograft tumors are shown. C. Body weight of nude mice. D. Determination of tumor *LINC01021* expression by qRT-PCR for both the control and treatment groups. The data were expressed as mean ± SD. **, $P < 0.01$. E. Western blot analysis of the protein expression of P53 and Bcl-2 in control or Da0324-treated mouse xenograft tumors. GAPGH was used as an internal control. F. Tumor volume of subcutaneous xenograft mouse models using KATO III cells treated with *LINC01021*-specific ASO or ASO-control. Tumor volume as measured by caliper of *LINC01021*-specific ASO or ASO-control (250 nmol/kg, intratumoral injection at three-day intervals) administered for 24 days in a subcutaneous xenograft model. The data were expressed as mean ± SD. *, $P < 0.05$. G. Tumors were excised after 24 days of treatment. Images and weight of the dissected xenograft tumors are shown. The data were expressed as mean ± SD. **, $P < 0.01$. H. Body weight of nude mice from ASO-control and ASO-*LINC01021* treatment groups. I. Determination of *LINC01021* expression by qRT-PCR in ASO-control and ASO-*LINC01021* treatment xenografts. *, $P < 0.05$. J. Western blot analysis of the protein expression of P53 and Bcl-2 in tumor tissues from ASO-control and ASO-*LINC01021* treatment groups. GAPGH was used as an internal control. ASO-ctrl, ASO-control; qRT-PCR, quantitative reverse transcription-polymerase chain reaction.

Simultaneously, P53 protein level was increased and Bcl-2 protein level was decreased in the ASO-*LINC01021* group relative to the ASO-control group (**Figure 6J**).
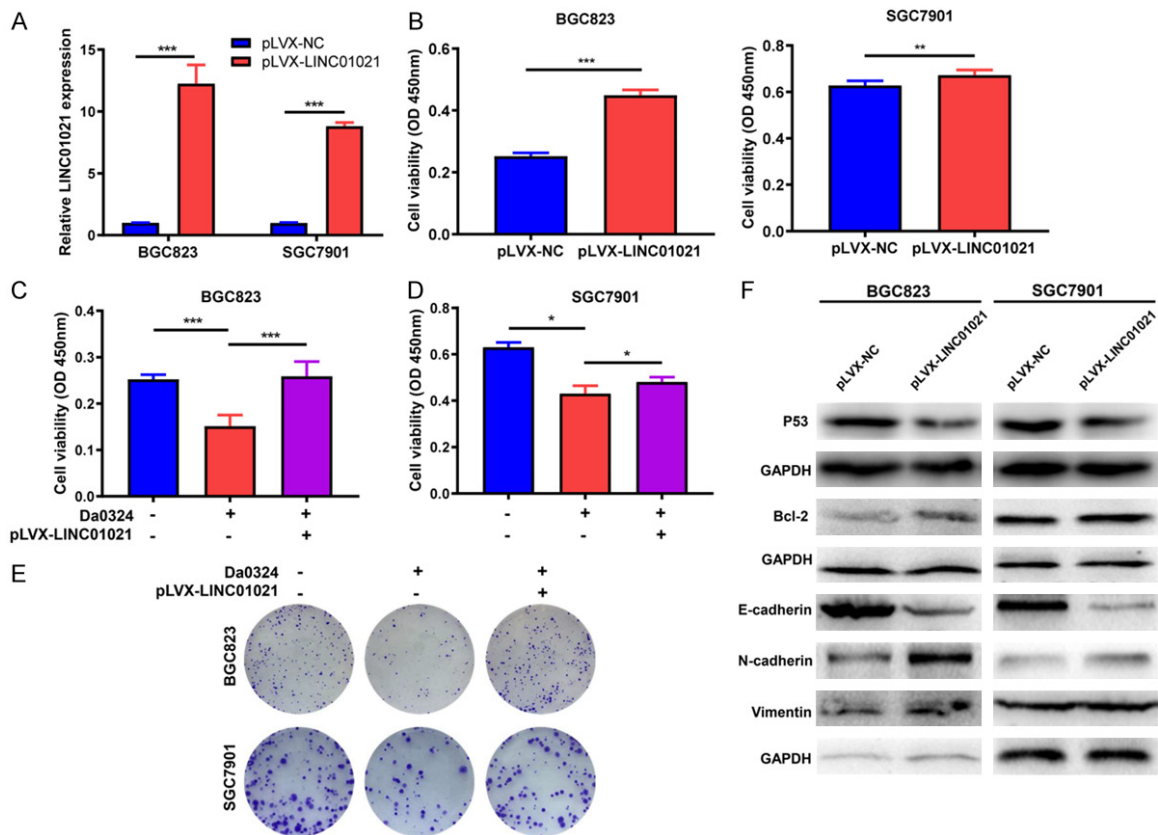
Figure 7. Overexpression of *LINC01021* reverses Da0324-mediated cytotoxic effects in gastric cancer cells. A. BGC823 and SGC7901 cells were transfected with negative control vector (pLVX-NC) or overexpressing *LINC01021* vector (pLVX-*LINC01021*) for 48 h. *LINC01021* expression was determined by qRT-PCR analysis. The data represent the mean ± SD from three independent experiments. ***, $P < 0.001$. B. BGC823 and SGC7901 cells were transfected with pLVX-NC or pLVX-*LINC01021* for 48 h. Cell viability was evaluated by CCK-8 assays. The data represent the mean ± SD from three independent experiments. **, $P < 0.01$; ***, $P < 0.001$. C, D. Overexpression of *LINC01021* reversed Da0324-mediated growth inhibition of gastric cancer cells. BGC823 and SGC7901 cells were transfected with pLVX-NC or pLVX-*LINC01021* for 24 h and then treated with Da0324 (4 μM) for 24 h. Cell viability was determined by CCK-8 assays. The data represent the mean ± SD from three independent experiments. *, $P < 0.05$; ***, $P < 0.001$. E. BGC823 and SGC7901 cells transfected with pLVX-NC or pLVX-*LINC01021* were exposed to Da0324 for 48 h and colony formation was assessed. F. BGC823 and SGC7901 cells were transfected with pLVX-NC or pLVX-*LINC01021* for 48 h and the expression levels of P53, Bcl-2, E-cadherin, N-cadherin and vimentin were determined by western blot analysis. GAPGH was used as an internal control. qRT-PCR, quantitative reverse transcription-polymerase chain reaction.

Overexpression of LINC01021 reverses Da0324-mediated cytotoxic effects in GC cells

To clarify whether *LINC01021* is involved in the inhibitory effect of Da0324 on GC cells, we established BGC823 and SGC7901 cell lines with stably overexpressed *LINC01021 via* lentiviral infection. This overexpression was verified by qRT-PCR (**Figure 7A**) and significantly promoted the growth of BGC823 and SGC7901 cells (**Figure 7B**). Further *in vitro* cell viability and colony formation assays showed that overexpression of *LINC01021* reversed the Da0324-mediated growth inhibition of BGC823 and SGC7901 cells (**Figure 7C-E**). As shown in

Figure 7F, overexpression of *LINC01021* also inhibited P53 protein expression and increased Bcl-2 protein expression in both cell lines. Moreover, overexpression of *LINC01021* induced EMT in both cell lines, evidenced by the epithelial marker E-cadherin expression being downregulated and the mesenchymal marker N-cadherin upregulated (**Figure 7F**). These findings support the role of *LINC01021* in Da0324-mediated cytotoxicity in GC cells.

Discussion

The use of natural compounds in cancer treatment is a hot research area, and studies have

reported successful use of some plant extracts and pure compounds to treat various cancers [29, 30]. Considering that curcumin is a safe and cost-effective natural agent with multiple targets in cancer, it is a suitable drug for exploring in the context of cancer treatment and can bring enormous clinical benefits [31]. However, the poor systemic bioavailability of curcumin hinders its therapeutic potential. In our previous study, we reported a novel curcumin analog, Da0324, which exhibited significantly improved stability and anti-cancer activity against GC cells *in vitro* and reduced toxicity to normal gastric mucous epithelial cells [26]. In this report, we further showed that Da0324 inhibited cell proliferation and colony formation of BGC823, SGC7901, and KATO III cell lines in a dose-dependent manner. Also, we discovered that Da0324 induced apoptosis and autophagy, as well as inhibited migration, invasion, and EMT in GC cells. Moreover, Da0324 significantly suppressed tumor growth of human GC xenografts *in vivo*.

Numerous studies have demonstrated that lncRNAs play important roles in cancer development [32]. In GC, dysregulation of lncRNAs is a common event and has been shown to affect tumor progression [33, 34]. LncRNAs may be potential targets for cancer therapy development [35]. During recent years, curcumin has been explored for potential in regulating lncRNAs [36]. For example, curcumin inhibits the Wnt and mTOR pathways in A549 cells through downregulation of the lncRNA *UCA1* [37]. Curcumin has also been reported to sensitize pancreatic cancer cells to gemcitabine by inhibiting expression of the lncRNA *PVT1* [38]. Furthermore, Esmatabadi et al. observed that dendrosomal curcumin (DNC) is an activator for GAS5, which decreases the chemotherapeutic effect of DNC in breast cancer cells [39], and Zamani et al. found that DNC increases expression of the lncRNA gene MEG3 in hepatocellular cancer, thereby impeding cancerous tumult [40].

To investigate the role of lncRNAs in the anti-cancer activity of Da03242, we performed high-throughput sequencing to identify lncRNAs differentially expressed in Da03242-treated GC cells. Interestingly, we found that Da0324 downregulated *LINC01021*, also named *PURPL* (P53 upregulated regulator of P53 levels), which is a direct P53 target [41]. *LINC01021*

has also been reported to inhibit the basal level of P53 by binding to MYBBP1A, a protein that binds and activates P53 [41]. There have been reports that knockdown of *LINC01021* increases the sensitivity of the colorectal cancer cell line HCT116 to chemotherapeutic drugs [42]. Although *LINC01021* plays an important role in colorectal cancer and liver cancer, little is known about the functionality of this lncRNA in GC [43]. In our study, we found that ASO-mediated silencing of *LINC01021* inhibited cell proliferation and induces apoptosis and autophagy in GC cells. We also found that *LINC01021*-specific ASO inhibits GC cell migration, invasion, and EMT, as well as the tumor growth of human GC xenografts *in vivo.* These results suggest that *LINC01021* may be a promising target for future GC treatment.

P53 is well known as a tumor suppressor gene involved in diverse metabolic processes [44]. More than 50% of tumors in humans have lost the protection of P53, resulting in resistance to apoptosis and infinite proliferation [45]. Furthermore, the proto-oncogene Bcl-2 is a key factor in inhibiting apoptosis and a p53 target [46]. Previous studies showed that curcumin activates P53 and downregulates Bcl-2 expression in some cancer cells [47-49]. In this study, we observed that Da0324 treatment or silencing of *LINC01021* also led to increased P53 expression and decreased Bcl-2 expression in GC cells both *in vitro* and *in vivo*. Conversely, overexpression of *LINC-01021* inhibited P53 expression and increased Bcl-2 expression in GC cells, as well as inducing EMT. Moreover, overexpression of *LINC01021* significantly promoted GC cell growth and reversed the Da0324-mediated cytotoxic effects, suggesting that Da0324 exerts anticancer effects by regulating *LINC-01021*, which can modulate the expression of P53 and Bcl-2.

In conclusion, our results demonstrate that Da0324 exerts anticancer activities against GC *via* downregulation of *LINC01021*, which leads to inhibition of the growth, migration, invasion, and EMT of GC cells and to increased cell apoptosis and autophagy through activation of P53. *LINC01021* is expected to be a new candidate for the treatment of GC. These findings reveal a novel anti-cancer mechanism of Da0324 a potential therapeutic target in the form of *LINC01021* for the treatment of GC.

Disclosure of conflict of interest

None.

Abbreviations

ASO, Antisense oligo; cDNA, complementary DNA; EMT, Epithelial-mesenchymal transition; FBS, fetal bovine serum; GC, gastric cancer; LC3B, light chain3B; lncRNA, Long non-coding RNA; p-mTOR, phosphorylated mTOR.

Address correspondence to: Dr. Rong Jin, Department of Epidemiology, The First Affiliated Hospital of Wenzhou Medical University, Wenzhou, China; Department of Gastroenterology, The First Affiliated Hospital of Wenzhou Medical University, Wenzhou, China. E-mail: jinrongjrjr@163.com; Dr. Lei Jiang, Central Laboratory, The First Affiliated Hospital of Wenzhou Medical University, Wenzhou 325000, China. Tel: +86-577-55579127; Fax: +86-577-55578999; E-mail: jiangleistone79@163.com

References

[1] Torre LA, Bray F, Siegel RL, Ferlay J, Lortet-Tieulent J and Jemal A. Global cancer statistics, 2012. CA Cancer J Clin 2015; 65: 87-108.

[2] Hayakawa Y, Sethi N, Sepulveda AR, Bass AJ and Wang TC. Oesophageal adenocarcinoma and gastric cancer: should we mind the gap? Nat Rev Cancer 2016; 16: 305-318.

[3] El-Sedfy A, Brar SS and Coburn NG. Current role of minimally invasive approaches in the treatment of early gastric cancer. World J Gastroenterol 2014; 20: 3880-3888.

[4] Liu H, Chen X, Sun J, Gao P, Song Y, Zhang N, Lu X, Xu H and Wang Z. The efficacy and toxicity of paclitaxel plus S-1 compared with paclitaxel plus 5-FU for advanced gastric cancer: a PRISMA systematic review and meta-analysis of randomized controlled trials. Medicine (Baltimore) 2014; 93: e164.

[5] Holohan C, Van Schaeybroeck S, Longley DB and Johnston PG. Cancer drug resistance: an evolving paradigm. Nat Rev Cancer 2013; 13: 714-726.

[6] Wagner AD, Grothe W, Haerting J, Kleber G, Grothey A and Fleig WE. Chemotherapy in advanced gastric cancer: a systematic review and meta-analysis based on aggregate data. J Clin Oncol 2006; 24: 2903-2909.

[7] Mattick JS and Rinn JL. Discovery and annotation of long noncoding RNAs. Nat Struct Mol Biol 2015; 22: 5-7.

[8] Tay Y, Rinn J and Pandolfi PP. The multilayered complexity of ceRNA crosstalk and competition. Nature 2014; 505: 344-352.

[9] Atianand MK, Caffrey DR and Fitzgerald KA. Immunobiology of long noncoding RNAs. Annu Rev Immunol 2017; 35: 177-198.

[10] Gutschner T and Diederichs S. The hallmarks of cancer: a long non-coding RNA point of view. RNA Biol 2012; 9: 703-719.

[11] Rinn JL, Kertesz M, Wang JK, Squazzo SL, Xu X, Brugmann SA, Goodnough LH, Helms JA, Farnham PJ, Segal E and Chang HY. Functional demarcation of active and silent chromatin domains in human HOX loci by noncoding RNAs. Cell 2007; 129: 1311-1323.

[12] Toiber D, Leprivier G and Rotblat B. Long noncoding RNA: noncoding and not coded. Cell Death Discov 2017; 3: 16104.

[13] Geisler S and Coller J. RNA in unexpected places: long non-coding RNA functions in diverse cellular contexts. Nat Rev Mol Cell Biol 2013; 14: 699-712.

[14] Kopp F and Mendell JT. Functional classification and experimental dissection of long noncoding RNAs. Cell 2018; 172: 393-407.

[15] Fanelli GN, Gasparini P, Coati I, Cui R, Pakula H, Chowdhury B, Valeri N, Loupakis F, Kupcinskas J, Cappellesso R and Fassan M. Long-noncoding RNAs in gastroesophageal cancers. Noncoding RNA Res 2018; 3: 195-212.

[16] Bhan A, Soleimani M and Mandal SS. Long noncoding RNA and cancer: a new paradigm. Cancer Res 2017; 77: 3965-3981.

[17] Nobili S, Lippi D, Witort E, Donnini M, Bausi L, Mini E and Capaccioli S. Natural compounds for cancer treatment and prevention. Pharmacol Res 2009; 59: 365-378.

[18] Priyadarsini KI. The chemistry of curcumin: from extraction to therapeutic agent. Molecules 2014; 19: 20091-20112.

[19] Karimian MS, Pirro M, Majeed M and Sahebkar A. Curcumin as a natural regulator of monocyte chemoattractant protein-1. Cytokine Growth Factor Rev 2017; 33: 55-63.

[20] Cavaleri F. Presenting a new standard drug model for turmeric and its prized extract, curcumin. Int J Inflam 2018; 2018: 5023429.

[21] Panahi Y, Saadat A, Beiraghdar F and Sahebkar A. Adjuvant therapy with bioavailability-boosted curcuminoids suppresses systemic inflammation and improves quality of life in patients with solid tumors: a randomized dou-

ble-blind placebo-controlled trial. Phytother Res 2014; 28: 1461-1467.

[22] Panahi Y, Alishiri GH, Parvin S and Sahebkar A. Mitigation of systemic oxidative stress by curcuminoids in osteoarthritis: results of a randomized controlled trial. J Diet Suppl 2016; 13: 209-220.

[23] Momtazi AA, Shahabipour F, Khatibi S, Johnston TP, Pirro M and Sahebkar A. Curcumin as a microRNA regulator in cancer: a review. Rev Physiol Biochem Pharmacol 2016; 171: 1-38.

[24] Gupta SC, Patchva S and Aggarwal BB. Therapeutic roles of curcumin: lessons learned from clinical trials. AAPS J 2013; 15: 195-218.

[25] Shetty D, Kim YJ, Shim H and Snyder JP. Eliminating the heart from the curcumin molecule: monocarbonyl curcumin mimics (MACs). Molecules 2014; 20: 249-292.

[26] Jin R, Xia Y, Chen Q, Li W, Chen D, Ye H, Zhao C, Du X, Shi D, Wu J and Liang G. Da0324, an inhibitor of nuclear factor-kappaB activation, demonstrates selective antitumor activity on human gastric cancer cells. Drug Des Devel Ther 2016; 10: 979-995.

[27] Zuo Z, Zhang P, Lin F, Shang W, Bi R, Lu F, Wu J and Jiang L. Interplay between Trx-1 and S100P promotes colorectal cancer cell epithelial-mesenchymal transition by up-regulating S100A4 through AKT activation. J Cell Mol Med 2018; 22: 2430-2441.

[28] Tanida I, Ueno T and Kominami E. LC3 and autophagy. Methods Mol Biol 2008; 445: 77-88.

[29] Talib WH. Regressions of breast carcinoma syngraft following treatment with piperine in combination with thymoquinone. Sci Pharm 2017; 85: 27.

[30] Talib WH. Consumption of garlic and lemon aqueous extracts combination reduces tumor burden by angiogenesis inhibition, apoptosis induction, and immune system modulation. Nutrition 2017; 43-44: 89-97.

[31] Bordoloi D and Kunnumakkara AB. The potential of curcumin: a multitargeting agent in cancer cell chemosensitization. Role of Nutraceuticals in Chemoresistance to Cancer 2018; 31-60.

[32] Huarte M. The emerging role of lncRNAs in cancer. Nat Med 2015; 21: 1253-1261.

[33] Song YX, Sun JX, Zhao JH, Yang YC, Shi JX, Wu ZH, Chen XW, Gao P, Miao ZF and Wang ZN. Non-coding RNAs participate in the regulatory network of CLDN4 via ceRNA mediated miRNA evasion. Nat Commun 2017; 8: 289.

[34] Sun TT, He J, Liang Q, Ren LL, Yan TT, Yu TC, Tang JY, Bao YJ, Hu Y, Lin Y, Sun D, Chen YX, Hong J, Chen H, Zou W and Fang JY. LncRNA GClnc1 promotes gastric carcinogenesis and may act as a modular scaffold of WDR5 and KAT2A complexes to specify the histone modi-

fication pattern. Cancer Discov 2016; 6: 784-801.

[35] Jiang MC, Ni JJ, Cui WY, Wang BY and Zhuo W. Emerging roles of lncRNA in cancer and therapeutic opportunities. Am J Cancer Res 2019; 9: 1354-1366.

[36] Mishra S, Verma SS, Rai V, Awasthee N, Chava S, Hui KM, Kumar AP, Challagundla KB, Sethi G and Gupta SC. Long non-coding RNAs are emerging targets of phytochemicals for cancer and other chronic diseases. Cell Mol Life Sci 2019; 76: 1947-1966.

[37] Wang WH, Chen J, Zhang BR, Lu SJ, Wang F, Peng L, Dai JH and Sun YZ. Curcumin inhibits proliferation and enhances apoptosis in A549 cells by downregulating lncRNA UCA1. Pharmazie 2018; 73: 402-407.

[38] Yoshida K, Toden S, Ravindranathan P, Han H and Goel A. Curcumin sensitizes pancreatic cancer cells to gemcitabine by attenuating PRC2 subunit EZH2, and the lncRNA PVT1 expression. Carcinogenesis 2017; 38: 1036-1046.

[39] Esmatabadi MJD, Motamedrad M and Sadeghizadeh M. Down-regulation of lncRNA, GAS5 decreases chemotherapeutic effect of dendrosomal curcumin (DNC) in breast cancer cells. Phytomedicine 2018; 42: 56-65.

[40] Zamani M, Sadeghizadeh M, Behmanesh M and Najafi F. Dendrosomal curcumin increases expression of the long non-coding RNA gene MEG3 via up-regulation of epi-miRs in hepatocellular cancer. Phytomedicine 2015; 22: 961-967.

[41] Li XL, Subramanian M, Jones MF, Chaudhary R, Singh DK, Zong X, Gryder B, Sindri S, Mo M, Schetter A, Wen X, Parvathaneni S, Kazandjian D, Jenkins LM, Tang W, Elloumi F, Martindale JL, Huarte M, Zhu Y, Robles AI, Frier SM, Rigo F, Cam M, Ambs S, Sharma S, Harris CC, Dasso M, Prasanth KV and Lal A. Long noncoding RNA PURPL suppresses basal p53 levels and promotes tumorigenicity in colorectal cancer. Cell Rep 2017; 20: 2408-2423.

[42] Kaller M, Gotz U and Hermeking H. Loss of p53-inducible long non-coding RNA LINC01021 increases chemosensitivity. Oncotarget 2017; 8: 102783-102800.

[43] Fu X, Wang Y, Wu G, Zhang W, Xu S and Wang W. Long noncoding RNA PURPL promotes cell proliferation in liver cancer by regulating p53. Mol Med Rep 2019; 19: 4998-5006.

[44] Bieging KT, Mello SS and Attardi LD. Unravelling mechanisms of p53-mediated tumour suppression. Nat Rev Cancer 2014; 14: 359-370.

[45] Kim S and An SS. Role of p53 isoforms and aggregations in cancer. Medicine (Baltimore) 2016; 95: e3993.

[46] Fischer M. Census and evaluation of p53 target genes. Oncogene 2017; 36: 3943-3956.

[47] He YC, He L, Khoshaba R, Lu FG, Cai C, Zhou FL, Liao DF and Cao D. Curcumin nicotinate selectively induces cancer cell apoptosis and cycle arrest through a P53-mediated mechanism. Molecules 2019; 24: 4179.

[48] Talib WH, Al-Hadid SA, Ali MBW, Al-Yasari IH and Ali MRA. Role of curcumin in regulating p53 in breast cancer: an overview of the mechanism of action. Breast Cancer (Dove Med Press) 2018; 10: 207-217.

[49] Yang J, Cao Y, Sun J and Zhang Y. Curcumin reduces the expression of Bcl-2 by upregulating miR-15a and miR-16 in MCF-7 cells. Med Oncol 2010; 27: 1114-1118.